

Dynamics of Transition from Static to Kinetic Friction

O. M. Braun,¹ I. Barel,² and M. Urbakh²

¹*Institute of Physics, National Academy of Sciences of Ukraine, 03028 Kiev, Ukraine*

²*School of Chemistry, Tel Aviv University, 69978 Tel Aviv, Israel*

(Received 29 June 2009; published 6 November 2009)

We propose a model for a description of dynamics of cracklike processes that occur at the interface between two blocks prior to the onset of frictional motion. We find that the onset of sliding is preceded by well-defined detachment fronts initiated at the slider trailing edge and extended across the slider over limited lengths smaller than the overall length of the slider. Three different types of detachment fronts may play a role in the onset of sliding: (i) Rayleigh (surface sound) fronts, (ii) slow detachment fronts, and (iii) fast fronts. The important consequence of the precursor dynamics is that before the transition to overall sliding occurs, the initially uniform, unstressed slider is already transformed into a highly nonuniform, stressed state. Our model allows us to explain experimental observations and predicts the effect of material properties on the dynamics of the transition to sliding.

DOI: 10.1103/PhysRevLett.103.194301

PACS numbers: 46.55.+d, 46.50.+a, 81.40.Pq

Interfacial friction is one of the oldest problems in physics and chemistry and certainly one of the most important from a practical point of view. Because of its practical importance and the relevance to basic scientific questions, there has been a major increase in the activity of the study of friction during the past decades [1–6]. In spite of the growing efforts, many aspects of friction are still not well understood. One of the aspects that has been somewhat overlooked is the onset of sliding motion. Understanding the dynamics of the transition to sliding is central to many different fields of physics and material science including tribology [1–6], performance of micro electromechanical systems [7,8], mechanics of fracture, and earthquakes [9–11].

Recent experimental studies of friction between two blocks (the slider and track) with an extended rough interface have shown that the onset of sliding is preceded by a discrete sequence of cracklike precursors initiated at shear levels that are well below the threshold for static friction [12–14]. It has been found that the transition to sliding is governed by the interplay between three types of fronts: sub-Rayleigh, intersonic, and slow fronts [13,14].

In this Letter we propose a model for a description of dynamics of cracklike processes that occur at the interface between two blocks prior to the onset of frictional motion. Our model allows us to explain experimental observations [13,14] and predicts the effect of material properties on the dynamics of the transition to sliding.

The model, shown schematically in Fig. 1, describes a typical tribological setup as explored, e.g., in experiments [13,14]. A slider of total mass M moves over an immobile rigid substrate (the track). The slider is pushed from its trailing edge (the left side) with a constant velocity V_d through a spring of elastic constant K_d . The experimentally measured spring force F corresponds to the friction force, and it is monitored in the simulation. In order to incorpo-

rate elasticity of the slider, we split it into N rigid blocks coupled by springs of the elastic constant $K_b = (N - 1)K$ so that the slider rigidity is K . This approach is similar to that proposed in the Burridge-Knopoff spring-block model of earthquakes [15], that has been further developed in a number of studies [16,17]. However, contrary to most earthquake models where phenomenological laws have been introduced to describe a friction at the slider-track interface, here we explicitly include interactions between each slider's block and the track through an array of “surface contacts” [18–22]. In the case of dry friction between rough surfaces these contacts represent interfacial asperities, while for lubricated friction they mimic patches of solidified lubricant or its domains.

Each contact connects the block and the track through a spring of the elastic constant k_i , where $i = 1, 2, \dots, N_s$, and N_s is the number of contacts between the block and track. The frictional dynamics is governed by two competing processes: (i) formation of contacts (junctions) between the block and the track that tends to inhibit sliding and (ii) rupture of contacts, i.e., detachment of springs from the block, a process that helps sliding. As long as a contact is intact, the contact's spring elongates or shortens with the velocity of the corresponding block. Therefore, the block experiences from the interface the force $-f = \sum_{i=1}^{N_s} f_i$, where $f_i = k_i l_i$ and $l_i(t)$ is the spring length. This force has to be added to the elastic forces acting from the left and right neighboring blocks. The description should be supplemented by the laws that govern rupture and

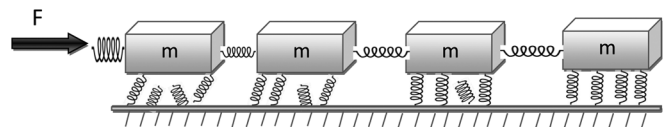


FIG. 1. Schematic sketch of a model setup.

formation of contacts. We assume that as long as the force f_i is below a certain threshold, f_{si} , corresponding to plastic flow of the entangled asperity, or to local melting of the boundary lubrication layer, this contact moves together with the corresponding block. When the force exceeds the threshold, the contact detaches from the slider and attaches again to the block in unstressed state (i.e., with the length $l_i = 0$) after some delay time τ . Thus, with every contact we associate the threshold value, f_{si} , which takes random values from a Gaussian distribution with the mean value $f_s = F_s/(NN_s)$ and a standard deviation Δf_s , where NN_s is a total number of contacts between the slider and track. It should be noted that the rupture threshold force f_{si} is proportional to the area A_i of the given contact, while the transverse rigidity k_i is proportional to the contact's size, $k_i \propto \sqrt{A_i}$. Therefore, the distribution of the contact's spring constants is coupled to the distribution of threshold forces by the relationship $k_i = \langle k \rangle (f_{si}/f_s)^{1/2}$, where $\langle k \rangle$ is the mean value of the contact spring constants. When the contact is reattached to the slider, we assign new values of the parameters f_{si} and k_i to the newborn contact.

Finally, in order to avoid artificial vibrations of the blocks, we introduce a viscous damping force with a coefficient η for the block motion relative to the track, $f_\eta = -m\eta\dot{x}_j$, where x_j is the coordinate of the center of mass of the j th block and $m = M/N$ is its mass. We note that the block's oscillations may also be damped due to internal friction within the blocks, i.e., due to phonon excitations inside the slider. The simulations show, however, that the dynamics of transition to sliding is insensitive to a particular choice of the damping force.

The behavior of a single block interacting with a track through an array of surface contacts has been studied previously [20–22]. Here we focus on a collective motion of the chain of interacting blocks. Although the calculations have been performed for a wide range of the model parameters, in what follows we present results only for a particular set of parameters: $K_d = 4 \times 10^6$ N/m, $M = 11.5$ kg, $F_s = 1.92 \times 10^3$ N, $K = 1.56 \times 10^7$ N/m, $V_d = 0.3$ mm/s, and $\eta = 0.005$ s⁻¹, $\Delta f_s/f_s = 0.05$, $\tau = 0.005$ s. The values of macroscopic parameters K_d , M , F_s , K , and V_d have been chosen in accordance with the experimental conditions in Refs. [13,14]. As for the interface rigidity, $K_s = N_s\langle k \rangle$, we present results for two cases: (i) a soft interface with $K_s = K$ (Fig. 2) and (ii) a stiff interface with $K_s = 50$ K (Fig. 3). The interface stiffness and mean rupture threshold force are expected to be directly related to the applied normal load. Most simulations have been done for 70 blocks ($N = 70$) and 100 contacts between each block and the track ($N_s = 100$).

Initially, before the experiment started, the slider is unstressed, the contacts are intact, and the entire interface is pinned. When the force is applied at the trailing edge of the slider, the shear stress accumulates in a finite region near the loading point. The solution of 1D elastic equations shows that displacements of the blocks, x_j , from their

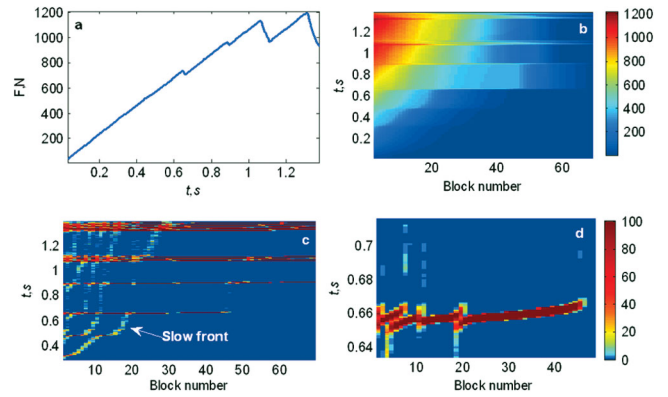


FIG. 2 (color). Onset of sliding for soft surface contacts, $K_s = K$. Panel (a) shows a loading curve, $F(t)$. Panels (b),(c) present color maps for the distribution of elastic forces, $K(N-1) \times (x_j - x_{j-1})$, in the slider and the fraction of attached contacts as functions of the block number j and time t . Panel (d) presents an enlarged view of the fast detachment front from (c) showing an excitation of secondary Rayleigh fronts by the slow fronts. The unstressed and stressed regions (b) and the regions with attached and detached contacts (c),(d) are displayed by blue and red colors. The bars to the right of the maps set up a correspondence between the colors and the values of the force in Newton (b) and the fraction of detached contacts in % (c).

equilibrium positions, x_j^0 , and the corresponding contractions of the springs connecting the blocks, $x_j - x_{j+1}$, decrease exponentially with a distance from the trailing edge, x_0 , namely, $x_j - x_j^0 \propto \exp[-\sqrt{K_s/NK}j]$. Thus, the length of the stressed region is determined by the ratio of the contact and slider stiffnesses, K_s/K . The exponential distribution of the shear stress along the slider is characteristic for the 1D model employed here, while a 3D description of the slider leads to a power law decrease of the stress [23]. Nevertheless, the localization of the shear stress in a finite range at the trailing edge that results from the 1D descrip-

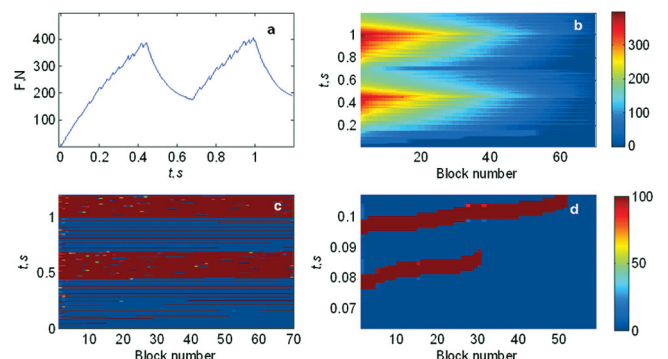


FIG. 3 (color). Onset of sliding for stiff surface contacts, $K_s = 50$ K. Panel (a) shows a loading curve, $F(t)$. Panels (b),(c) present color maps for the distribution of elastic forces, $K(N-1) \times (x_j - x_{j-1})$, in the slider and the fraction of attached contacts as functions of the block number j and time t . Panel (d) presents an enlarged view of the detachment front from (c) showing a propagation of a Rayleigh front. The notation is as in Fig. 2.

tion is consistent with the experimental configuration [13,14] where the finite spatial extent of the stressed region is determined by a height at which the force is applied.

As the applied force is increased, the stress in this region grows until it exceeds the thresholds for the rupture of surface contacts, f_{si} , and a detachment front starts to propagate across the interface (see Figs. 2 and 3). The manifestation of the detachment fronts is seen in the loading curves, $F(t)$, presented in Figs. 2(a) and 3(a) which show a sequence of small drops in $F(t)$. These drops correspond to discrete cracklike precursors to sliding which occur well below the onset of overall motion and result from a minute motion of blocks at the slider trailing edge (see Fig. 4).

In order to understand the nature of the detachment fronts and their effect on the state of the system we present in Figs. 2 and 3 the 2D maps for a stress distribution along the chain of blocks [Figs. 2(b) and 3(b)] and for a fraction of detached contacts [Figs. 2(c) and 3(c)] as functions of the block number and time. For a wide range of parameters we found that the onset of sliding is preceded by well-defined detachment fronts which are initiated at the trailing edge and extend over limited lengths across the slider that are smaller than its overall length. Figures 2(c) and 3(c) show that these fronts generate a strongly nonuniform stress distribution across the slider. As a result, a new detachment front will propagate into an already highly stressed region that has been prepared by the previous front. The new front easily ruptures the prestressed contacts in this region, further extends itself, and causes further elastic deformation of the slider. The threshold values of the applied force corresponding to the detachment fronts are considerably lower than the value needed to initiate overall motion of the slider, because only regions of limited length are fractured during these precursor events.

In accordance with experimental observations [13,14] we found that three different types of detachment fronts may play a role in the onset of sliding: (i) Rayleigh (surface sound) fronts, (ii) slow detachment fronts, and (iii) fast

fronts. In our simulations the precursors to sliding are always initiated at the trailing edge by the Rayleigh front that rapidly accelerates until approaching the sound velocity, $V \propto \sqrt{K/M}$. This front is characterized by a simultaneous motion of a number of blocks which are detached from the track (i.e., all surface contact of these blocks is ruptured). Therefore, the velocity of the front V is determined by the elasticity of the slider and independent of the stiffness and rupture thresholds of the surface contacts. The properties of the contacts influence a length scale of the slider domain (number of blocks) involved in a simultaneous motion, and the local displacements of the blocks that decrease with the ratio between the stiffnesses of the surface contacts and the slider, K_s/K (see Fig. 4). Figure 4 also shows that during transition to sliding the blocks perform stick-slip motion where slips correspond to the precursor events, and the slip lengths are in the micrometer range. One can also see that creep motion of the blocks takes place at forces below the contact rupture forces, as it was recently observed in experiments with steel and silicon [6].

Once the Rayleigh front extends beyond the high-stressed region, it stops; however, an excess strain accumulates at the tip of the arrested front. We found that for moderately flexible surface contacts, $K_s \approx K$, this excess stress can trigger a slow detachment front propagating with a velocity that is over an order of magnitude lower than that of the Rayleigh waves [see Fig. 2(b)]. In contrast to the Rayleigh fronts which exhibit the collective motion of the detached blocks, the slow fronts represent the motion of individual blocks. At each moment only one or few blocks are partially detached from the track and moves. As a result the velocity of the slow front is mostly determined by the properties of the individual block (stiffness of surfaces contacts, thresholds of rupture forces) and only slightly depends on the slider elasticity. In particular, the velocity decreases with the increase in interfacial stiffness K_s and mean rupture force F_s . Our calculations demonstrate (see Fig. 3) that for stiff surface contacts with $K_s = 50$ K the

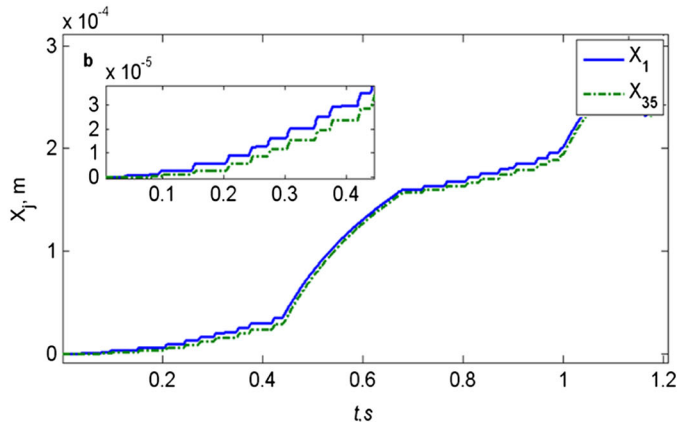
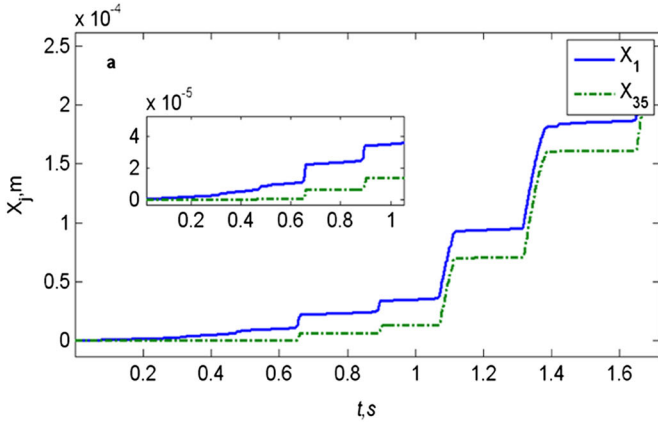


FIG. 4 (color online). Displacements of the first block x_1 (trailing edge) and the middle block x_{35} as a function of time for the case of soft (a) and stiff (b) surface contacts. Insets present enlarged views of the motion of blocks prior to the onset of overall sliding.

slow fronts do not evolve, since in this case the excess stress accumulated at the tip of the arrested Rayleigh front cannot overcome the resistance of the surface contacts and initiate slow motion.

Figures 2(b) and 2(d) show that the interaction between the Rayleigh front propagating from the trailing edge and the slow fronts triggers the excitation of secondary Rayleigh fronts at various distances from the edge. This effect leads to a formation of a new type of fast fronts which correspond to a superposition of Rayleigh fronts initiated simultaneously at different locations across the slider. An effective velocity of such fast fronts can be a few times higher than the Rayleigh wave speed. We did not find the fast fronts in the case of stiff surface contacts [see Figs. 3(b) and 3(d)] where slow fronts could not be excited.

Figures 2(c) and 3(c) demonstrate that, with each successive detachment front, the stress distribution across the slider becomes increasingly more nonuniform. By the time the system is ready to slide, the precursor fronts have generated a highly stressed state of the slider and the contacts. Hence, the transition to sliding occurs in the highly nonuniform, stressed system. The transition to sliding is manifested by a significant drop in the loading curve, $F(t)$, that is an order of magnitude larger than the small drops corresponding to the precursors of sliding. Contrary to the precursors which are caused by the discrete detachment fronts, the transition to overall sliding occurs through a quasicontinuous (in time) set of fronts propagating one after another from the trailing to the leading edges of the slider. During the time interval corresponding to this transition most surface contacts are simultaneously detached which allows the overall motion of the slider.

It is notable that for the system with moderately flexible surface contacts ($K_s \approx K$) the nonuniform stress distribution produced by the sequence of detachment fronts prior to the first sliding event remains virtually unchanged in the subsequent stick-slip motion. This result is consistent with experimental observations [13,14] which suggested that nonuniformity of the contact is the preferred state of the system during sliding. However, according to our calculations, in the case of stiff surface contacts the high stresses relieved by sliding and the nearly uniform state of the slider is renewed. The difference in stress relaxation during the stick-slip transition leads to a very different mechanism of stick-slip motion for soft and stiff surface contacts. In the case of soft contacts the second and subsequent stick-slip events occur at the prestressed interface and do not involve a sequence of cracklike precursors [see Figs. 2 and 4(a)]. This also has been found in the experiments [13,14]. In the case of stiff contacts where the stress is relieved by sliding, all stick-slip transitions occur through the excitation of discrete detachment fronts [see Figs. 3 and 4(b)]. Thus dynamics of transition from static to kinetic friction

strongly depends on the ratio between the stiffnesses of the surface contacts and the slider, K_s/K .

We grateful to J. Fineberg, S. M. Rubinstein, and E. Bouchbinder for helpful discussions. O. B. acknowledges hospitality at the School of Chemistry, Tel Aviv University. The work, as part of the European Science Foundation EUROCORES Program FANAS (CPRs ACOF and AQUALUBE), was supported by the Israel Science Foundation (773/05) and the EC Sixth Framework Program ERASCT-2003-980409.

-
- [1] B. N. J. Persson, *Sliding Friction: Physical Principles and Applications* (Springer-Verlag, Berlin, 1998).
 - [2] M. H. Muser, M. Urbakh, and M. O. Robbins, *Adv. Chem. Phys.* **126**, 187 (2003).
 - [3] M. Urbakh *et al.*, *Nature (London)* **430**, 525 (2004).
 - [4] O. M. Braun and A. G. Naumovets, *Surf. Sci. Rep.* **60**, 79 (2006).
 - [5] T. Baumberger and C. Caroli, *Adv. Phys.* **55**, 279 (2006).
 - [6] Z. Yang, H. P. Zhang, and M. Marder, *Proc. Natl. Acad. Sci. U.S.A.* **105**, 13 264 (2008).
 - [7] *Springer Handbook of Nano-Technology*, edited by B. Bhushan (Springer, Berlin, 2007), 2nd ed., Chap. 29–45.
 - [8] A. D. Corwin and M. P. de Broer, *Appl. Phys. Lett.* **84**, 2451 (2004).
 - [9] A. Cochard and J. R. Rice, *J. Geophys. Res. [Solid Earth]* **105**, 25 891 (2000).
 - [10] Y. Ben-Zion, *J. Mech. Phys. Solids* **49**, 2209 (2001).
 - [11] K. Xia, A. J. Rosakis, and H. Kanamori, *Science* **303**, 1859 (2004).
 - [12] T. Baumberger, C. Caroli, and O. Ronsin, *Phys. Rev. Lett.* **88**, 075509 (2002).
 - [13] S. M. Rubinstein, G. Cohen, and J. Fineberg, *Nature (London)* **430**, 1005 (2004).
 - [14] S. M. Rubinstein, G. Cohen, and J. Fineberg, *Phys. Rev. Lett.* **98**, 226103 (2007).
 - [15] R. Burridge and L. Knopoff, *Bull. Seismol. Soc. Am.* **57**, 341 (1967).
 - [16] J. M. Carlson and J. M. Langer, *Phys. Rev. Lett.* **62**, 2632 (1989).
 - [17] Z. Olami, H. J. S. Feder, and K. Christensen, *Phys. Rev. Lett.* **68**, 1244 (1992).
 - [18] B. N. J. Persson, *Phys. Rev. B* **51**, 13 568 (1995).
 - [19] O. M. Braun and J. Röder, *Phys. Rev. Lett.* **88**, 096102 (2002).
 - [20] A. E. Filippov, J. Klafter, and M. Urbakh, *Phys. Rev. Lett.* **92**, 135503 (2004).
 - [21] O. M. Braun and M. Peyrard, *Phys. Rev. Lett.* **100**, 125501 (2008).
 - [22] O. M. Braun and E. Tosatti, *Europhys. Lett.* (to be published).
 - [23] L. D. Landau and E. M. Lifshitz, *Theory of Elasticity*, Course of Theoretical Physics Vol. 7 (Pergamon, New York, 1986).